

Studying the Impact of Stochasticity on the Evaluation of Deep Neural Networks for Forest-Fire Prediction

Harshit Kumar, Biswadeep Chakraborty, Beomseok Kang, Saibal Mukhopadhyay
Georgia Institute of Technology
Atlanta, Georgia, USA

ABSTRACT

This paper presents the first systematic study of Deep Neural Network (DNN) evaluation under stochastic assumptions, focusing on wildfire prediction. We note that current evaluation strategies emphasize a DNN’s replication of observed ground truths rather than its ability to learn the underlying stochastic processes, crucial for capturing wildfire evolution’s complexity. To bridge this gap, we propose a novel evaluation criterion: Has the DNN learned the stochastic process? Using a synthetic dataset, we introduce a framework to characterize the stochastic process (generated by randomness in fire evolution rules). Through this framework, we assess an evaluation metric’s capability to test if the DNN has learned the stochastic process. Our findings show that conventional metrics, including classification-based metrics and proper scoring rules, are inadequate. We identify the Expected Calibration Error (ECE) as a robust metric that tests the proposed evaluation criteria, offering asymptotic guarantees of proper scoring rules and improved interpretability through calibration curves. We extend our analysis to real-world wildfire data, highlighting the limitations of traditional evaluation methods and demonstrating the utility of ECE as a stochasticity-compatible metric alongside existing ones.

KEYWORDS

physical systems, stochasticity, deep learning, evaluation, wildfire

1 INTRODUCTION

DNNs have become a preferred tool for data-driven modeling of *physical systems* across various fields such as fluid dynamics [37], cosmology [41], economics [3], and neuroscience [17]. A critical application area is wildfire prediction, where the need for improved forecasts is driven by the growing frequency and severity of wildfires [39, 45]. Leveraging the broad spatial and temporal coverage of remote sensing data from satellites [16] and aircraft-based sensors [4], DNN models are trained to capture fire evolution dynamics. These DNNs surpass traditional modeling approaches [32], offering significant improvements in wildfire management strategies. The DNNs take observations of fire evolution over various time steps—ranging from 24 hours to a year—as input and predict fire-map evolution for future time steps, from one day to 30 days ahead, for predicting whether specific locations will burn [16, 32, 48].

A fundamental characteristic of physical systems is stochasticity. For example, wildfires, characterized by their unpredictable evolution [23], can be modeled as a *stochastic process*. Here, ground truth (GT) is conceptualized as a distribution, represented by a random variable (RV) Z_t , indexed by time t . Under this interpretation, DNNs in existing studies [16, 18, 32, 48] learn from one set of random realizations (training data) and are evaluated on another (test data), each sampled from a distinct stochastic process. Prevailing

evaluation strategy implicitly assumes that the observed GT is the sole outcome, due to the practical constraint of observing a single realization of the stochastic process, identified here as a *deterministic bias*. Implications of such stochastic interpretations on wildfire modeling (and physical systems in general) is unexplored.

In this paper, we focus on evaluating DNNs that model stochastic systems like wildfire evolution. Evaluation is a crucial step guiding the development and selection of DNN models [6]. Unlike the extensive research on DNN model development, evaluation, particularly under stochastic assumptions, remains an underexplored area. Current evaluation criteria emphasizes replicating observed GT, rather than a DNN’s ability to learn the stochastic process. A significant challenge is the stochastic process’s *unobservability*, with only single realizations accessible. Therefore, we ask two research questions: [RQ1] *Why is it critical to evaluate a DNN’s ability to learn the stochastic process?* [RQ2] *How do we evaluate whether a DNN has successfully learned the stochastic process?*

To address our questions, we propose a new evaluation criterion: *Has the DNN learned the stochastic process?* For thorough testing, we introduce a synthetic benchmark containing varying levels of stochasticity, and a stochastic framework to characterize the high-dimensional stochastic process of forest fire evolution. This framework includes two scales: Micro RV $M_{t,(x,y)}$ for agent-level details (representing individual trees’ states) and Macro RV Z_t to capture the system’s overall state (reflecting the forest’s condition). Utilizing this benchmark and framework, we assess the proposed criterion with two prevalent metric classes: classification-based (e.g., Recall, AUC-PR) and scoring-rule-based (e.g., MSE). Our findings highlight shortcomings in existing evaluation methods, particularly their unreliability in highly stochastic situations. To mitigate this, we identify ECE as an effective metric that meets our evaluation criterion, offering asymptotic reliability and improved interpretability through calibration curves. Our key contributions are:

- To address RQ1, we develop a stochastic framework to characterize forest-fire as a stochastic process with system variance $Var(Z_t)$. We demonstrate that current evaluation criteria, focused on fidelity to observed ground truth, shows high variance in scenarios with elevated $Var(Z_t)$, highlighting their unreliability and underscoring the need for a new stochasticity-compatible evaluation criterion.
- For RQ2, we show that ECE exclusively evaluates whether the DNN has learned the stochastic interactions guiding system evolution. This application of ECE differs from its conventional use for assessing uncertainty estimate quality.
- We extend our study to the recently released real-world wildfire dataset, "Next Day WildFire Spread" [16], demonstrating the limitations of current evaluation metrics and the utility of the proposed evaluation criterion.

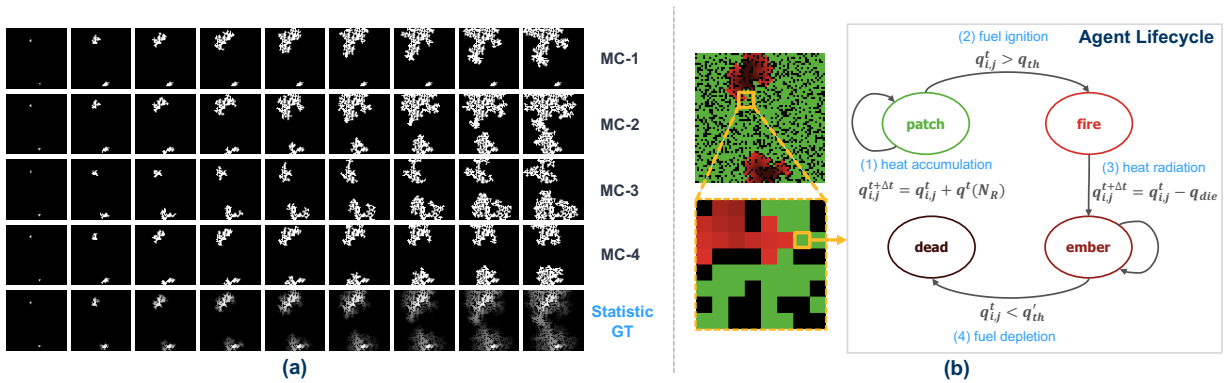


Figure 1: (a) The first four rows display four distinct realizations (MC simulations) of fire evolution from the same initial condition (fire seed location). The last row shows the Statistic-GT of fire evolution, with each pixel representing the Bernoulli distribution parameter from which the realizations are sampled from; (b) [Left] Snapshot of forest-fire evolution in NetLogo using a 64x64 grid of agents, [Right] Flowchart depicting a single agent’s evolution rules inspired from Rothermel’s model [34].

Table 1: Selected works in Wildfire Prediction

Work	Window Size	DNN	Evaluation Metric
[32]	Observation: T Prediction: T+24h	CNN	F1-score, Recall, Accuracy
[48]	Observation: [T-52w, T] Prediction: T+5w	CNN+LSTM	AUC-ROC, MSE
[16]	Observation: T Prediction: T+24h	CNN	AUC-PR, Precision, Recall

Table 2: Conventional Evaluation Metrics and Descriptions

Metric	Description
Precision	Proportion of true positive predictions among all positive predictions
Recall	Proportion of true positive predictions among all actual positive instances
Accuracy	Proportion of correct predictions among all predictions
F1-score	Harmonic mean of precision and recall
AUC-PR	Area under the precision-recall curve, evaluating trade-off between precision and recall
AUC-ROC	Area under the receiver operating characteristic curve, evaluating trade-off between true positive rate and false positive rate
MSE	Mean squared error, measuring average squared difference between predicted and actual values

The paper is organized as follows: §2 presents background and related work. §3 details our proposed stochastic process-based framework. In §4, we conduct benchmark experiments using this framework and address the two key research questions. We apply our insights to a real-world wildfire dataset in §5. The discussion and conclusions are in §6 and §7, respectively.

2 BACKGROUND AND RELATED WORK

2.1 Formulation of Wildfire Modeling

Formally, wildfire evolution can be modeled on a grid of size $H \times W^1$, where each grid-cell (i, j) at time t is denoted by a binary random variable $M_{t,(i,j)}$, indicating fire presence (1) or absence (0). Let $X_t \in \{0, 1\}^{H \times W}$ encapsulate the fire occurrence status across all cells at

¹ $H = W = 64$ in our work.

time t . Additionally, let $O_{t,(i,j)} \in \mathbb{R}^n$ represent an n -dimensional vector of observational variables (e.g., vegetation, terrain, weather conditions) for each cell at time t , used by DNNs like those in [16]. The goal is to predict the joint conditional distribution of fire occurrences across the grid from time $t + 1$ to T , utilizing both past fire maps and observational variables, formally given by:

$$P(X_{t+1}, \dots, X_T | X_1, \dots, X_t, O_1, \dots, O_t), \quad (1)$$

where X_1, \dots, X_t denote the observed fire maps from the initial time to time t , O_1, \dots, O_t are the corresponding observational variables, and X_{t+1}, \dots, X_T are the forecasted fire maps up to time T .

DNN-based modeling of Wildfires. Conventional modeling tools, such as FARSITE [7], have high operational costs due to reliance on ground-based data collection. The growing application of DNNs in wildfire prediction, especially with remote sensing data, is evident in key studies [16, 32, 48] summarized in Table 1 and reviewed comprehensively in [18]. For example, FireCast [32] outperforms traditional models by 20% in predicting 24-hour wildfire perimeters using satellite imagery [7] (see §B.1 for a taxonomy on wildfire models). These DNNs integrate various covariates like vegetation, terrain, and weather conditions; for example, Huot et al. use a 64 x 64-pixel grid, each containing 11 observational variables [16]. DNNs operate in two phases for wildfire prediction: learning fire evolution rules during observation, and applying this knowledge for future predictions. DNNs are trained using Binary Cross Entropy (BCE) loss. Post-training, the DNNs are evaluated using evaluation metrics [6] summarized in Table 2².

2.2 Stochasticity in Wildfire Evolution

Stochastic Dynamics in Wildfire Modeling and Challenges. Stochasticity plays a central role in wildfire evolution [23]. It emerges from the interaction of various components—vegetation, terrain, weather conditions, and human activities (e.g., fire suppression efforts). The subtle variations in interactions can lead to significantly divergent outcomes from a given state, a phenomenon akin to the “butterfly effect” [24]. These factors add noise to the rules

²AUC-ROC is not recommended for fire map prediction due to class imbalance [16, 35].

of fire evolution that DNNs aim to learn. Despite its prevalence and significance, the influence of stochasticity has been largely overlooked in traditional deterministic approaches to wildfire modeling. Real-world data limitations, typically presenting only a single outcome from a range of possibilities, obscure the true nature of stochastic interactions. This gap limits the understanding of stochastic systems and hinders research into how stochasticity affects DNN-based modeling of real-world wildfire scenarios.

To address the limitations of real-world datasets, we create a synthetic forest-fire dataset using cellular automata-based models that simulate a wide spectrum of outcomes (see Appendix B.2 for applications of cellular automata in wildfire modeling). In our work, we utilize an agent-based model called NetLogo [40], to implement a CA-based forest fire model. In the Agent-based formulation of Forest Fire evolution, each pixel on a spatial grid (similar to remote sensing data), is treated as an agent. Agents interact with neighbors (in the Moore neighborhood) using stochastic rules (simulated using NetLogo). The local interactions collectively drive the global fire evolution, often manifesting in complex, fractal-like patterns (see Figure 1.b). This approach allows us to study the stochastic dynamics at play in wildfire evolution, offering insights that are unconfined by the limitations of real-world data.

3 FOREST FIRE AS A STOCHASTIC PROCESS

We characterize Forest Fire as a stochastic process to understand its complexity and motivate evaluating this aspect, answering RQ1.

3.1 Simulating a Wildfire as a Stochastic Process

A stochastic process characterizes the dynamic and unpredictable evolution of physical systems over time, and is represented by a sequence of random variables $Z_1, Z_2, \dots, Z_t, \dots$, [31]. To empirically generate the stochastic process, we develop a NetLogo-based Forest-Fire model. We first establish deterministic interaction rules for neighboring agents (shown in Figure 1.b), and then add stochastic noise in the interactions (Details in Appendix C.1). To make the rules stochastic, we introduce p_{ignite} , the probability of fire after ignition conditions are met (i.e., $q > q_{\text{threshold}}$). In deterministic scenarios, p_{ignite} is set to 100, ensuring ignition once the threshold is reached. A p_{ignite} value of 95 indicates a 95% chance of ignition under the same conditions. The *S-Level* parameter is defined as $(1 - p_{\text{ignite}}) \times 100$, with higher *S-Level* values indicating more randomness in agent interactions, and an *S-Level* of 0 corresponding to deterministic interactions.

Empirical Stochastic Process (ESP). We represent an ESP using 1000 Monte Carlo (MC) simulations, each initiated with identical conditions (fire seed and forest configuration) and run until fuel depletion. This approach ensures variations in fire evolution stem exclusively from stochastic interactions. Figure 1.a depicts four distinct realizations of forest fire evolution (MC-1 to 4) from the same starting point. Finally, we execute a sweep of the *S-Level* parameter, creating an ESP for each *S-Level* parameter.

3.2 Micro and Macro Random Variable

Addressing the challenge of modeling high-dimensional wildfire evolution, we leverage insights from statistical mechanics [5] to adopt a dual-scale modeling approach. At the microscopic level,

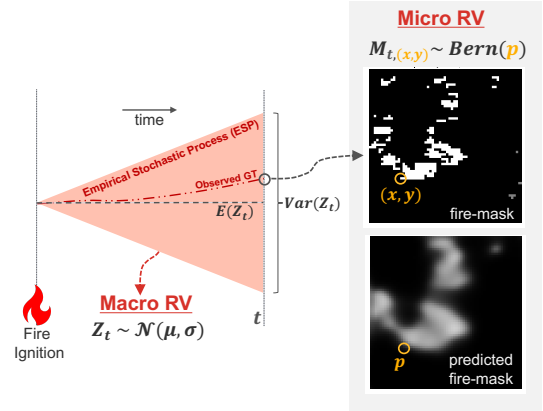


Figure 2: Illustrates the stochastic framework with Macro and Micro Random Variables (RVs) for forest fire evolution. The ESP (shaded in red) consists of 1000 Monte-Carlo (MC) Simulations, generated using a cellular-automata model.

individual agent behavior is captured through the Micro Random Variable (RV), $M_{t,(x,y)}$, while at the macroscopic level, the collective system behavior is represented by the Macro RV, Z_t .

Micro-Level Modeling of the Stochastic Process. At the micro level, each grid point (x, y) at time t is modeled using a Micro RV, $M_{t,(x,y)}$, which follows a Bernoulli distribution with an expectation $E[M_{t,(x,y)}]$ equal to its probability p . The ensemble of Micro RVs across the grid, denoted as $\{M_{t,(x,y)} | 1 \leq x \leq H, 1 \leq y \leq W\}$, represents the grid-level micro representation of fire evolution. This Micro RV Map represents GT of the statistic, and termed *Statistic-GT*. In practical scenarios, a single realization (represented by one MC simulation) of the stochastic process (represented by the *Statistic-GT*) is observable. Parameters for each Micro RV are derived from the ESP by normalizing the burn frequency of each pixel at each timestep, across the MC simulations.

Macro-Level Modeling of the Stochastic Process. The Macro RV, Z_t , represents the collective state of the system at time t . Formally, we define Z_t as the sum of the Micro RVs across the grid:

$$Z_t = \sum_{x=1}^H \sum_{y=1}^W M_{t,(x,y)} \quad (2)$$

Applying the Central Limit Theorem (due to the large number of Micro RVs $\approx 10^3$), Z_t can be effectively modeled using a Normal distribution, characterized by its mean $E[Z_t]$ and variance $Var[Z_t]$. Sampling from Z_t provides a macro-state value, representing the aggregate state of all agents. It should be noted that multiple microstates can correspond to the same macrostate value. The parameters of the Macro RV is extracted from the ESP by recording the number of unburnt trees (macrostate) at each time step and creating a distribution at each time step using the 1000 MC simulations, from which we directly compute the mean and variance.

The fifth row in Figure 1. (a) displays the Micro RV map for the ESP at *S-Level* 20, where each pixel’s value, $E[M_{t,(x,y)}]$, indicates the burn probability at that location and time, conditioned on the initial fire seed and forest configuration. Figure 2 summarizes the proposed framework for characterizing the stochastic process.

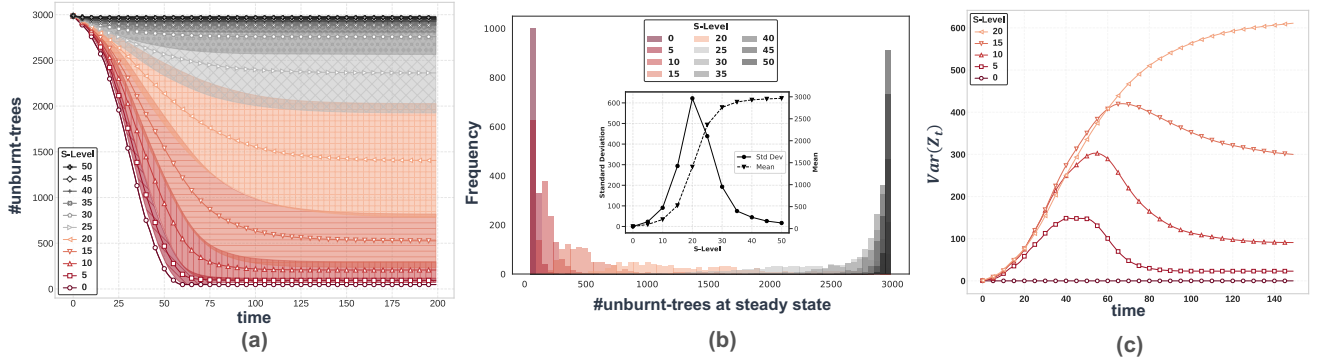


Figure 3: Characterizes the Macro RV Z_t : (a) ESP representing Z_t across different S-Levels; (b) Histogram of Z_t at steady state across S-Levels, with an inset showing trends in $E[Z_t]$ and $Var[Z_t]$; (c) $Var[Z_t]$ as a function of time fore selected test-cases.

3.3 Characterizing the S-Level Test Cases

Figure 3. (a) shows the Macro RV Z_t over time with colors changing from red (S-Level=0) to black (S-Level=50) in increments of 5. The central line and shaded areas denote $E[Z_t]$ and $Var[Z_t]$. Figure 3.(b) presents histograms representing Z_t at steady state for different S-Levels, with inset showing mean and standard deviation (SD) at each level. Figure 3.(c) displays $Var[Z_t]$ over time for select S-Levels used in our study.

Key observations include: At S-Level 0 (deterministic), the absence of SD implies a singular evolutionary path, an assumption implicit in current remote-sensing-based wildfire modeling [16, 18, 48]. As S-Level increases, $Var[Z_t]$ peaks at S-Level 20, indicative of a chaotic system with multiple fire evolution pathways, aligning with real-world fire behavior [23]. The $Var[Z_t]$ indicates the system’s tendency towards exploring diverse macrostates, with increasing variance indicating greater unpredictability.

Implications for evaluation. As observed through $Var[Z_t]$, the potential state space that a system with stochastic interactions can explore is vast, yet typically only a single realization is observed. An appropriate evaluation strategy should not solely judge a DNN’s performance based on its replication of the observed GT, since a DNN may still accurately model Z_t without replicating the exact observed GT. An effective evaluation strategy should also focus on whether a DNN has captured the stochastic interactions (S-Level), indicative of its understanding of the stochastic process.

4 BENCHMARK EXPERIMENTS

Using S-Level Test Cases, we examine in §4.3 how the current evaluation focus impacts the reliability of metrics, justifying the need for new stochasticity-compatible evaluation criteria (RQ1). We then show in §4.4 how ECE effectively assesses whether the DNN has learned the stochastic interactions (RQ2).

4.1 Evaluation Metrics used in this study

Classification-based metrics. Precision, Recall, F1-score, and AUC-PR are favored for their ability to delineate type-1 and type-2 errors. These metrics are standard in DNN-based forest fire prediction due to the binary nature of fire spread outcomes and the direct link between each forecast and a decision-making action, critical in high-risk scenarios.

Scoring Rules. Metrics like MSE evaluate probabilistic forecasts and are formally known as scoring rules [12]. A proper scoring rule S ensures that the expected score, under the GT distribution D_{gt} , is minimized by an accurate forecast distribution D_f . Formally, for any forecast D_f , we have:

$$\mathbb{E}_{y \sim D_{gt}} [S(y, D_{gt})] \leq \mathbb{E}_{y \sim D_{gt}} [S(y, D_f)]. \quad (3)$$

A scoring rule is *strictly proper* if this minimum is unique, offering asymptotic guarantees that the best score corresponds to the forecast matching the GT distribution. However, limitations arise with finite samples, where scoring rules may not capture basic forecasting errors [27]. Scoring rules do not provide decision-based quantification of DNN’s performance (less interpretable), making them less favored in wildfire prediction [16, 32, 48].

Calibration Error. According to the Brier Score decomposition of the MSE [36], it splits into two components: Calibration Error and inherent outcome variability:

$$MSE = \underbrace{E[(E[O|F] - F)^2]}_{\text{Calibration Error}} + \underbrace{E[Var(O|F)]}_{Var(Z_t)} \quad (4)$$

The Calibration Error, $E[(E[O|F] - F)^2]$, measures the probabilistic accuracy of the forecast, while the second component, $E[Var(O|F)]$, quantifies the inherent uncertainty unexplained by the forecasts. By isolating the Calibration Error, we can specifically assess forecast accuracy, excluding the impact of $Var[Z_t]$. This error benefits from asymptotic guarantees and can be visualized through calibration curves, enhancing interpretability (see §C.2 for details on Calibration Curve). *Based on the Brier Score decomposition, we hypothesize that Calibration Error can effectively evaluate whether the DNN has learned the stochastic interactions.* We use the Expected Calibration Error (ECE) [29] in this study, a popular metric used for calculating calibration error:

$$ECE = \sum_{k=1}^m \frac{|I_k|}{N} |\text{acc}(I_k) - \text{conf}(I_k)| \quad (5)$$

Here, m represents the number of intervals, I_k the k -th interval of predicted probabilities, $|I_k|$ the number of grid location predictions in I_k , and N the total number of grid location predictions across all samples. The term $\text{acc}(I_k)$ indicates the accuracy within interval I_k , calculated as the proportion of correct predictions, and $\text{conf}(I_k)$ denotes the average predicted probability within that interval.

Application of ECE in Deep Learning vs. Our Work. ECE and calibration curves are commonly used in deep learning to measure the quality of uncertainty estimates [1]. Predictive uncertainty in traditional deterministic tasks like image classification manifests in two forms: data uncertainty from measurement errors and model uncertainty due to the model’s unfamiliarity with certain data points [26]. Unlike these uncertainties arising from limitations in the DNN pipeline, our work encounters aleatoric (irreducible) uncertainty, which stems from the macro variance inherent in the physical system. Our application of ECE assesses whether the DNN has accurately learned the stochastic interactions and the associated stochastic process, rather than just measuring the quality of predictive uncertainty, which, while still possible, is secondary to evaluating our proposed criteria.

4.2 DNN Training

We used convLSTM-CA, a modified convLSTM architecture that retains spatial information (see §D.1 for details on architecture choice). Our dataset contains 1,000 forest fire simulations with S-Levels from 0 (deterministic) to 20 (highly stochastic), in increments of 5. Each simulation, *unique* in fire seed and forest layout, represents a single realization of the stochastic process, mirroring real-world diversity. The DNNs train on one set of these realizations and are tested on another, providing a controlled environment that replicates practical training and evaluation scenarios. The training dataset, comprising 700 simulations, was segmented into 60-frame intervals. The DNN initially observes the first 10 frames in RGB, then predicts the next 50 frames using binary segmentation (1 for burnt, 0 for unburnt areas). We utilize BCE loss for training.

Calibration with the Statistic-GT. In Figure 4, we plot the mean Statistic-GT against the corresponding mean DNN Forecast. The correlation between them suggests that the DNN is effectively learning to predict the Statistic-GT (details in §D.3). This capability is linked to the use of BCE loss (a proper scoring rule), which promotes calibrated forecasts by teaching the DNN to learn the true probability distribution of the process [12]. The Statistic-GT, which represents the joint GT distribution (see Equation 1), robustly assesses whether the DNN is learning the agent interactions. In real-world applications, the Statistic-GT is inaccessible; only singular realizations sampled from it are observed. This limitation makes the evaluation process sensitive to the macro-variance of the system, which dictates the diversity of realizations the system can produce.

4.3 Impact of Macro-Variance on metrics

Methodology. Under RQ1, we further investigate the impact of $Var[Z_t]$ on currently used evaluation metrics: classification-based and scoring-rule. For this experiment, we perform inference on the DNN trained with S-Level 20, a setting that exhibits chaotic behavior typical of wildfire evolution. The test dataset comprises 1000 MC simulations of the S-Level 20 ESP test case, all with identical initial conditions. We calculate the evaluation metric independently for each timestep of each MC simulation. Each simulation at a given timestep t has a specific $Var[Z_t]$, reflecting macro-variance at that moment. We measure the Standard Deviation (SD) of the evaluation metric across the 1000 MC simulations against $Var[Z_t]$ to assess the metric’s sensitivity to macro-variance. Since all simulations

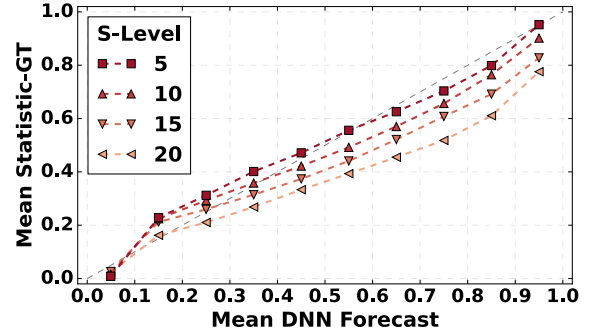


Figure 4: Shows the correlation between Statistic-GT and the DNN forecast, indicating that the DNN is learning to predict the statistic representing the stochastic process.

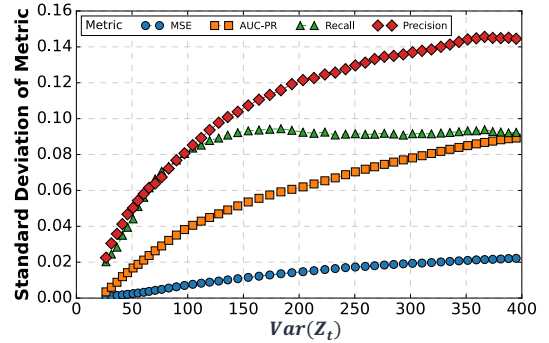


Figure 5: Shows the SD of the evaluation metrics vs. $Var[Z_t]$ for S-Level 20; higher SD indicates greater sensitivity to $Var[Z_t]$ and reduced reliability.

originate from the same stochastic process, an ideal metric should be faithful to the stochastic process, and demonstrate minimal sensitivity to individual realizations of the ESP. More detailed results using different S-Levels is in §E.

Results. Figure 5 shows the SD of evaluation metrics against $Var[Z_t]$. The significant increase in SD for classification-based metrics (Precision, Recall, AUC-PR) highlights their heightened sensitivity to macro-variance and reduced reliability. Precision and Recall suffer high variance in stochastic settings due to their reliance on thresholding, which can produce predictive outcomes misaligned with the actual GT. This issue stems from the incompatibility of "thresholding" with stochastic processes, extending beyond the common critique of arbitrary threshold selection, such as a 0.5 cutoff [8]. Although AUC-PR is less sensitive than other threshold-based metrics, it still encounters challenges from its integration of False Positives (FP) through Precision, where the traditional concept of FP loses relevance because any non-zero forecast by the DNN renders both outcomes (1 and 0) plausible. Conversely, MSE demonstrates less sensitivity to macro-variance due to its basis as a strictly proper scoring rule [12], ensuring greater resilience.

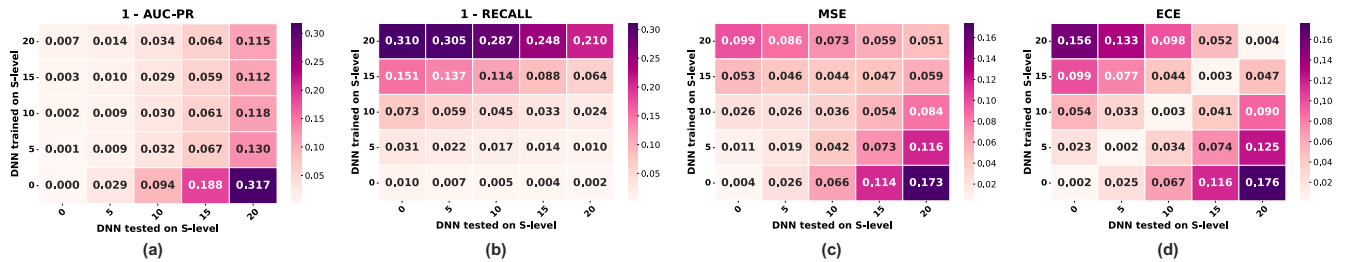


Figure 6: DNN trained on one S-Level, tested on another, evaluated by (a) $(1 - \text{AUC-PR})_{\downarrow}$, (b) $(1 - \text{Recall})_{\downarrow}$, (c) MSE_{\downarrow} , and (d) ECE_{\downarrow} . Diagonal behavior, evident in ECE, shows the metric’s ability to assess whether DNN has learned the stochastic process.

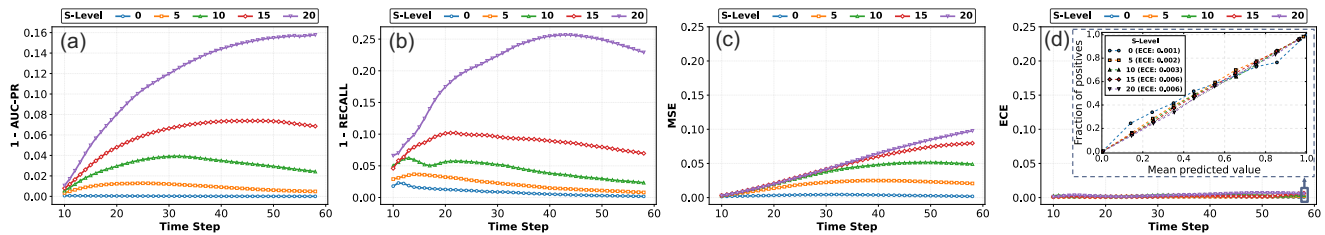


Figure 7: Long Horizon Performance of the DNN using (a) AUC-PR, (b) Recall, (c) MSE, and (d) ECE [calibration curve in inset].

4.4 Evaluating Fidelity to Stochastic Process

Methodology. To answer RQ2, we claim that ECE can faithfully evaluate whether a DNN has learned the stochastic process. To rigorously test this claim, we conduct an experiment using five different versions of DNNs designed in §4.2, each trained at a specific S-Level. We then evaluate each DNN across five test splits, each at a different S-Level. The goal is to determine the effectiveness of various evaluation metrics in assessing whether the DNN has learned the stochastic process. Ideally, an evaluation metric that accurately reflects this learning should perform best when the S-Level of the trained DNN matches the test split’s S-Level.

The results are shown in the matrix heatmap in Figure 6, one for each evaluation metric. The rows represent the evaluation scores for a DNN trained at a specific S-Level, and the columns show the scores for each test split at corresponding S-Levels. Distinct diagonal behavior is observed only in the ECE matrix, where optimal scores occur when the training S-Level matches the test S-Level. The MSE matrix shows some diagonal trends, but its measure of inherent stochasticity obscures this pattern. In contrast, the classification-based metrics, AUC-PR and Recall, exhibit no such pattern, indicating their ineffectiveness in assessing whether a DNN has learned the stochastic process. We extend these findings to other DNN architectures, including convLSTM variants (with spatial-bottleneck or multiple-layers) and AR-NCA [20], in §F and confirm that these observations are generally applicable.

DNN Prediction in Short vs. Long Horizon We provide additional evidence to support that ECE is effective for assessing the proposed evaluation criteria. Our hypothesis is that if the DNN has learned the stochastic interactions, then long-term predictions evaluated with ECE should remain stable as S-Level is constant during a simulation. Figure 7.a-c shows the performance of trained DNNs using AUC-PR, Recall, and MSE at the same S-Level test split (mirroring the diagonal in Figure 6). The evaluation score for each time step is calculated by aggregating predictions and GT across the

300 simulations in the test split. We observe that evaluation metrics decline as the S-Level increases and with longer prediction horizons. Despite the DNN having learned the stochastic process, mismatches with the observed realizations lead to declining scores. In Figure 7.d, the ECE scores show that long-term predictions measured by ECE are stable, indicating success in predicting the stochastic process. The inset calibration curve in Figure 7.d confirms the DNN’s calibrated predictions. Experimental confirmation shows that if DNN is trained and tested on different S-Levels, there is a noticeable drop in long-horizon performance reported by ECE (see §G).

Key Takeaway

Each class of evaluation metric measures a specific aspect:

- (1) classification-based metrics tests fidelity-to-realization (F2R),
- (2) scoring-rules tests fidelity-to-statistics (F2S),
- (3) ECE tests fidelity-to-the-stochastic-process (F2SP).

5 APPLICATION TO REAL WORLD WILDFIRE

Finally, we extend our study to a real-world wildfire dataset. Since this is real-world data, $\text{Var}[Z_t]$ cannot be calculated as only one realization of Z_t is observed, yet the system is highly stochastic. This section addresses two main themes: (1) addressing the disconnect between negative evaluation scores and positive qualitative observations discussed in the Next Day Wildfire Spread (NDWS) dataset [16], and (2) using multiple DNNs, we simulate scenarios to select the most suitable DNN. In this context, we discuss how ECE can complement existing metrics and guide the selection of DNNs.

5.1 Dataset and DNN Models used

Dataset. The NDWS dataset compiles historical wildfire incidents with 11 observational variables into two-dimensional regions with a 1 km resolution [16]. These variables include elevation, wind direction and speed, minimum and maximum temperature, humidity,

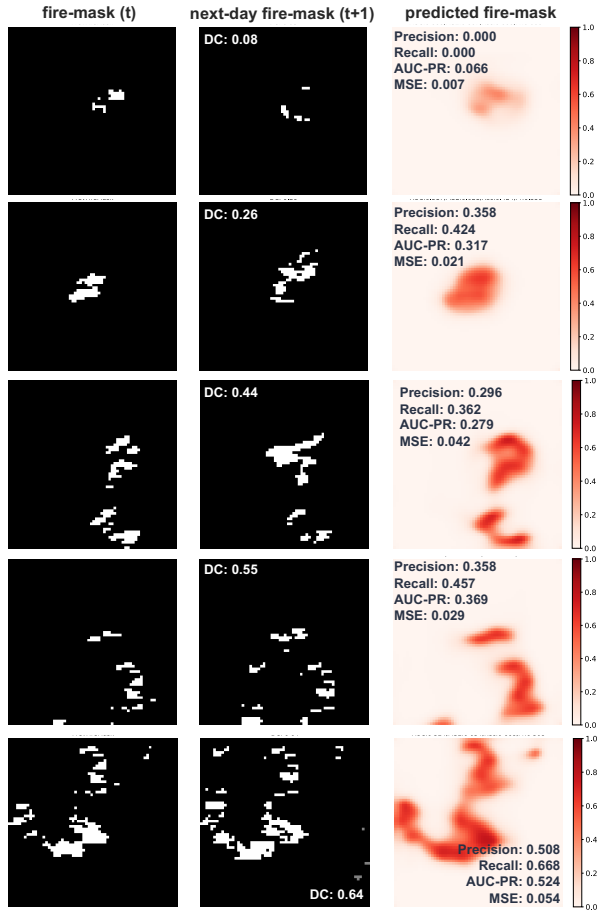


Figure 8: The DNN takes as input fire mask (left column) alongside 11 observational variables to forecast the next-day fire mask (right column), compared against the observed ground truth (GT) in the middle column. Evaluation through F2R metrics indicates suboptimal performance, whereas the MSE score, despite being low, does not adequately reflect the DNN’s practical efficacy.

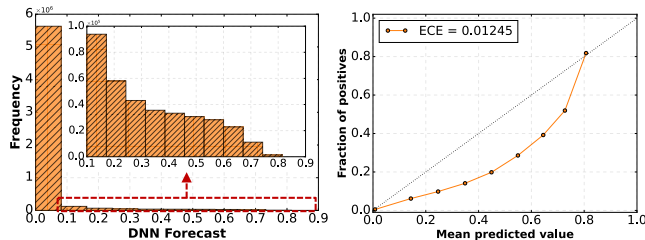


Figure 9: [Left] displays the distribution histogram of forecasts generated by Conv-AE; [Right] shows a Calibration Curve that illustrates forecast accuracy in an interpretable manner. This curve suggests (1) the DNN’s tendency towards overconfidence in mid-range forecasts, and (2) the accuracy of its probabilistic predictions is better for forecasts at the lower and upper ends of the probability spectrum.

precipitation, drought index, vegetation, population density, and the Energy Release Component (Details in §C.3). The dataset documents 18,545 wildfire events and provides sequential snapshots of fire spread, captured at time t and $t + 1$ day.

DNN Models. The DNNs take as input a spatial map of 11 observational variables and fire spread at time t , and predict the binary segmentation map for fire spread at time $t + 1$. We use five DNN architectures in this study. The first, Conv-AE, is a convolutional autoencoder model replicated from Huot et al.’s methodology [16]. The second, Conv-CA, modifies Conv-AE by removing the spatial bottleneck, which limits the mixing of global information (see Appendix D.1 for details). The third, AR-NCA, stands for Attentive Recurrent Neural Cellular Automata, designed for locally interacting discrete systems like forest fire evolution [20]. The fourth is SegFormer [47], a transformer-based segmentation model. The fifth is U-Net, a convolution-based image segmentation model [33].

5.2 Revisiting the Evaluation of Conv-AE [16]

Experiment. Huot et al. reported Conv-AE’s AUC-PR score of 0.284 over the test split. They acknowledged that “while the metrics on the positive class seem low,” qualitative visualizations demonstrated that “fires are predicted,” “predicted fires are roughly in the target location,” and there is “good recognition of larger fires” [16]. We make similar observations in Figure 8, which displays the fire mask at time t , the next-day fire mask at time $t + 1$ (observed GT), and the predicted forecast from Conv-AE. The low scores suggest poor performance, yet the qualitative insights suggest the opposite. We hypothesize that this disconnect stems from the highly stochastic nature of wildfires, which though unobservable, compromises the classification-based metrics used by the authors. Our aim is to re-evaluate the DNN’s predictions in light of our new insights.

Results and Discussion. Huot et al. reported overall scores for Precision, Recall, and AUC-PR. We use the DC calculated between the fire mask at time t and the next-day fire mask to quantify fire evolution. Evaluation scores stratified by DC values are presented in Table 3. Higher DC values indicate greater Fire Map (FM) overlap, signifying gradual fire progression, whereas lower values indicate abrupt changes. For instance, a DC of 0.08 in Figure 8 signifies a complete shift in the fire front, while a DC of 0.64 shows slower progression from time t to $t + 1$. The data in Table 3 show that all

Table 3: Evaluation Metrics for Conv-AE stratified by Dice Coefficient values measuring Fire Map Overlap (FMO) between t^{th} and $t + 1^{th}$ day. (\uparrow means higher is better)

FMO (DC)	Sup.	Precision \uparrow	Recall \uparrow	AUC-PR \uparrow	MSE \downarrow	ECE \downarrow
0.9-1.0	1	0.000	0.000	1.000	0.000	0.001
0.8-0.9	4	0.000	0.000	0.445	0.001	0.006
0.7-0.8	3	0.771	0.578	0.693	0.003	0.008
0.6-0.7	75	0.571	0.700	0.624	0.013	0.019
0.5-0.6	116	0.475	0.606	0.512	0.019	0.025
0.4-0.5	145	0.373	0.501	0.355	0.017	0.022
0.3-0.4	142	0.324	0.381	0.283	0.019	0.022
0.2-0.3	217	0.281	0.284	0.217	0.017	0.014
0.1-0.2	150	0.206	0.121	0.128	0.017	0.013
0.0-0.1	836	0.085	0.028	0.044	0.007	0.005
Overall	1689	0.346	0.311	0.247	0.012	0.012

metrics generally decrease as FM overlap decreases. However, lower MSE, ECE scores for small FM overlap indicates fewer probabilistic errors and better modeling of stochastic process by the DNN.

Figure 9 includes a histogram of the DNN’s predictions across the test split and a calibration curve, revealing overconfident predictions in the middle probability region but well-calibrated predictions at the extremes. For example, locations predicted to burn at $p = 0.80$ did indeed burn 80% of the time. This supports the DNN’s ability to faithfully learn the stochasticity in the fire map evolution, *addressing the disconnect* between positive observations and negative traditional evaluation scores in [16].

Table 4: Performance of DNNs on NDWS Dataset. Each DNN has a rank in (.) according to the respective evaluation metric.

DNN	AUC-PR \uparrow	MSE \downarrow	ECE \downarrow
Conv-AE [16]	0.2473 (5)	0.0124 (4)	0.0119 (4)
Conv-CA	0.2631 (4)	0.0146 (5)	0.0207 (5)
AR-NCA [20]	0.2790 (2)	0.0099 (2)	0.0012 (1)
SegFormer [47]	0.2727 (3)	0.0100 (3)	0.0020 (2)
U-Net [33]	0.3302 (1)	0.0096 (1)	0.0023 (3)

5.3 Conflict in DNN Rankings

Conflicts in model rankings are a vital component of model selection process [14]. We simulate a real-world scenario for selecting the optimal DNN starting from a candidate set of DNNs. We explore how ECE complements existing evaluation metrics and guides DNN selection. Table 4 displays the overall evaluation scores (AUC-PR, MSE, and ECE) for five different DNNs on the test split, *revealing rank conflicts among the metrics*. This raises a crucial question: Which evaluation metric most accurately reflects model performance, and which ranking should be trusted? As per our insight, each metric assesses different performance facets: AUC-PR measures F2R, MSE measures F2S, and ECE measures F2SP. The choice depends on the priorities of the intended application. For example, while MSE scores for AR-NCA, SegFormer, and U-Net are similar, the ECE for AR-NCA is about half that of the others. If prioritizing F2SP, AR-NCA would be the best choice. Conversely, if F2R is more critical, U-Net, with its competitive ECE, is preferable. The weighting relies on an estimate of system randomness. For highly random systems, F2S, F2SP are more reliable; F2R works better in low randomness. Ultimately, this study advocates for a multi-faceted evaluation approach, emphasizing F2SP as a crucial component.

6 DISCUSSION

Limitations of ECE in stochastic contexts. Asymptotic guarantees take effect after observing a sufficient number of samples (see §H). It also exhibits lower discriminative capabilities compared to classification-based metrics (see §F). As with most statistical measures, qualitative should always be inspected for context.

Related Works in Stochastic Video Prediction. While deterministic prediction is effective in predictable contexts (e.g., car movement on a straight trajectory), video prediction struggles with sporadic unpredictable events (e.g., car turning) [30]. In such cases,

deterministic DNNs predict an average of all possible outcomes, leading to blurry predictions [28]. Therefore, the focus is on developing stochastic DNNs that offer a range of potential outcomes with high contrast. This involves sampling from a learnt latent variable to generate diverse realizations. For evaluation, the authors report the best score across different generated samples, testing for *fidelity to realization* [15]. Unlike the sporadic nature of stochasticity in video prediction, wildfires exhibit stochasticity consistently [9]. This challenges the application of stochastic DNNs, which face issues of *uncontrollable* and variable quality predictions due to their focus on making high-contrast predictions [19], thereby making it a less suitable strategy for high-risk wildfire prediction. Our study diverges from traditional stochastic video prediction, emphasizing *fidelity to statistics/stochastic-process* as a more suitable strategy for high-risk wildfire prediction. By providing stochastic interpretation and stochasticity-compatible evaluation methods, we aim to enhance the reliability of DNNs in stochastic wildfire prediction.

Generalization to binary-classifications. The implications of our study extend beyond wildfire prediction, offering insights into the evaluation of DNNs across a spectrum of binary classification tasks within physical and social systems. Systems such as the spread of epidemics [11, 46] and the propagation of rumors in social networks [21, 42], characterized by dynamic elements and discrete state transitions, similarly exhibit complex global behaviors arising from simple local interactions. Our findings suggest that traditional evaluation metrics, which focus on fidelity to observed GT, may not adequately capture the DNN’s ability to learn the stochastic interactions present in the system. A low value of these metrics, while not desirable, does not necessarily indicate the DNN’s inability to learn the stochastic system. Instead, stochasticity-compatible metrics like MSE and ECE, which assess fidelity to statistical patterns, could offer more reliable and interpretable assessments.

7 CONCLUSION

In this paper, we propose a new evaluation criterion that exclusively assesses a DNN’s ability to learn the stochastic interactions governing forest fire evolution. We highlight that DNN pipelines have a deterministic bias and explore the impact of incorporating stochastic assumptions into the pipeline. We find that existing evaluation metrics lack reliability in highly stochastic scenarios and fail to assess fidelity to the stochastic process. Using the Brier Score decomposition, we identify ECE as a potential candidate for testing our criterion. We demonstrate that ECE effectively evaluates whether a DNN has learned the stochastic interactions. An interesting observation is that if the randomness in interactions remains constant, ECE shows that long-term prediction performance stays stable, contrasting with the portrayal by current metrics like AUC-PR and MSE. With a refined understanding of what each class of evaluation metric measures, we apply our insights to a real-world dataset. Here, we revisit the qualitative analysis by the original authors, addressing the disconnect between positive qualitative assessments and negative performance scores. We illustrate another utility of ECE in resolving conflicts in DNN rankings. Our work not only sheds light on the complexities of evaluating DNNs in stochastic systems but also paves the way for developing more robust and interpretable evaluation strategies for such systems.

ACKNOWLEDGMENTS

The authors thank Hemant Kumawat and Minah Lee for the insightful discussions. This work was supported in part by the Office of Naval Research under Grant N00014-20-1-2432. The views and conclusions contained in this document are those of the authors and should not be interpreted as representing the official policies, either expressed or implied, of the Office of Naval Research or the U.S. Government.

REFERENCES

- [1] Moloud Abdar, Farhad Pourpanah, Sadiq Hussain, Dana Rezazadegan, Li Liu, Mohammad Ghavamzadeh, Paul Fieguth, Xiaochun Cao, Abbas Khosravi, U. Rajendra Acharya, Vladimir Makarenkov, and Saeid Nahavandi. 2021. A review of uncertainty quantification in deep learning: Techniques, applications and challenges. *Information Fusion* 76 (Dec. 2021), 243–297. <https://doi.org/10.1016/j.inffus.2021.05.008>
- [2] Per Bak, Chao Tang, and Kurt Wiesenfeld. 1987. Self-organized criticality: An explanation of the $1/f$ noise. *Phys. Rev. Lett.* 59 (Jul 1987), 381–384. Issue 4. <https://doi.org/10.1103/PhysRevLett.59.381>
- [3] Richard H Day. 1994. Complex economic dynamics-vol. 1: An introduction to dynamical systems and market mechanisms. *MIT Press Books* 1 (1994).
- [4] Jigar Doshi, Dominic Garcia, Cliff Massey, Pablo Lluca, Nicolas Borensztein, Michael Baird, Matthew Cook, and Devaki Raj. 2019. FireNet: Real-time Segmentation of Fire Perimeter from Aerial Video. In *Neural Information Processing Systems 2019*. Available: <https://arxiv.org/abs/1910.06407>.
- [5] Peter Eastman. 2015. Introduction to Statistical Mechanics. <https://web.stanford.edu/~peastman/statmech/>. Accessed: [insert date of access].
- [6] C. Ferri, J. Hernández-Orallo, and R. Modroui. 2009. An experimental comparison of performance measures for classification. *Pattern Recognition Letters* 30, 1 (Jan. 2009), 27–38. <https://doi.org/10.1016/j.patrec.2008.08.010>
- [7] Mark A. Finney. 1998. *FARSITE: Fire Area Simulator-model development and evaluation*. Technical Report. <https://doi.org/10.2737/rmrs-rp-4>
- [8] Damien Fourure, Muhammad Usama Javaid, Nicolas Posocco, and Simon Tihon. 2021. Anomaly Detection: How to Artificially Increase Your F1-Score with a Biased Evaluation Protocol. In *Machine Learning and Knowledge Discovery in Databases. Applied Data Science Track (Lecture Notes in Computer Science)*, Yuxiao Dong, Nicolas Kourtellis, Barbara Hammer, and Jose A. Lozano (Eds.). Springer International Publishing, Cham, 3–18. https://doi.org/10.1007/978-3-030-86514-6_1
- [9] Robert G. Gallager. 2013. *Stochastic Processes: Theory for Applications*. Cambridge University Press. <https://doi.org/10.1017/CBO9781139626514>
- [10] Zhangyang Gao, Cheng Tan, Lirong Wu, and Stan Z Li. 2022. Simvp: Simpler yet better video prediction. In *Proceedings of the IEEE/CVF Conference on Computer Vision and Pattern Recognition*. 3170–3180.
- [11] Sayantari Ghosh and Saunik Bhattacharya. 2020. A data-driven understanding of COVID-19 dynamics using sequential genetic algorithm based probabilistic cellular automata. *Applied Soft Computing* 96 (2020), 106692.
- [12] Tilmann Gneiting and Adrian E Raftery. 2007. Strictly proper scoring rules, prediction, and estimation. *Journal of the American statistical Association* 102, 477 (2007), 359–378.
- [13] Joana Gouveia Freire and Carlos Castro DaCamara. 2019. Using cellular automata to simulate wildfire propagation and to assist in fire management. *Natural Hazards and Earth System Sciences* 19, 1 (Jan. 2019), 169–179. <https://doi.org/10.5194/nhess-19-169-2019>
- [14] Matthew J. Heaton, Abhirup Datta, Andrew Finley, Reinhard Furrer, Rajarshi Guhaniyogi, Florian Gerber, Robert B. Gramacy, Dorit Hammerling, Matthias Katzfuss, Finn Lindgren, Douglas W. Nychka, Furong Sun, and Andrew Zammit-Mangion. 2018. A Case Study Competition Among Methods for Analyzing Large Spatial Data. [arXiv:1710.05013 \[stat.ME\]](https://arxiv.org/abs/1710.05013)
- [15] Mikael Henaff, Junbo Zhao, and Yann LeCun. 2017. Prediction Under Uncertainty with Error-Encoding Networks. [arXiv:1711.04994 \[cs.AI\]](https://arxiv.org/abs/1711.04994)
- [16] Fantine Huot, R. Lily Hu, Nita Goyal, Tharun Sankar, Matthias Ihme, and Yi-Fan Chen. 2022. Next Day Wildfire Spread: A Machine Learning Dataset to Predict Wildfire Spreading From Remote-Sensing Data. *IEEE Transactions on Geoscience and Remote Sensing* 60 (2022), 1–13. <https://doi.org/10.1109/TGRS.2022.3192974>
- [17] Eugene M Izhikevich. 2007. *Dynamical systems in neuroscience*. MIT press.
- [18] Piyush Jain, Sean C.P. Coogan, Sriram Ganapathi Subramanian, Mark Crowley, Steve Taylor, and Mike D. Flannigan. 2020. A review of machine learning applications in wildfire science and management. *Environmental Reviews* 28, 4 (2020), 478–505. <https://doi.org/10.1139/er-2020-0019> [arXiv:https://doi.org/10.1139/er-2020-0019](https://arxiv.org/abs/2020.0019)
- [19] Beibei Jin, Yu Hu, Qiankun Tang, Jingyu Niu, Zhiping Shi, Yinhe Han, and Xiaowei Li. 2020. Exploring Spatial-Temporal Multi-Frequency Analysis for High-Fidelity and Temporal-Consistency Video Prediction. In *Proceedings of the IEEE/CVF Conference on Computer Vision and Pattern Recognition (CVPR)*.
- [20] Beomseok Kang, Harshit Kumar, Minah Lee, Biswadeep Chakraborty, and Saibal Mukhopadhyay. 2024. Learning Locally Interacting Discrete Dynamical Systems: Towards Data-Efficient and Scalable Prediction. [arXiv:2404.06460 \[eess.SY\]](https://arxiv.org/abs/2404.06460)
- [21] Kazuki Kawachi, Motohide Seki, Hiraku Yoshida, Yohei Otake, Katsuhide Warashina, and Hiroshi Ueda. 2008. A rumor transmission model with various contact interactions. *Journal of theoretical biology* 253, 1 (2008), 55–60.
- [22] Xingdong Li, Mingxian Zhang, Shiyu Zhang, Jiuqing Liu, Shufa Sun, Tongxin Hu, and Long Sun. 2022. Simulating Forest Fire Spread with Cellular Automaton Driven by a LSTM Based Speed Model. *Fire* 5, 1 (Jan. 2022), 13. <https://doi.org/10.3390/fire5010013>
- [23] Naian Liu, Jiao Lei, Gao Wei, Haixiang Chen, and Xiaodong Xie. 2021. Combustion dynamics of large-scale wildfires. *Proceedings of the Combustion Institute* 38 (01 2021). <https://doi.org/10.1016/j.proci.2020.11.006>
- [24] Edward Lorenz. 2000. The butterfly effect. *World Scientific Series on Nonlinear Science Series A* 39 (2000), 91–94.
- [25] K. Malarz, S. Kaczanowska, and K. Kulakowski. 2002. Are Forest Fires Predictable? *International Journal of Modern Physics C* 13, 08 (2002), 1017–1031. <https://doi.org/10.1142/S0129183102003760> [arXiv:https://doi.org/10.1142/S0129183102003760](https://arxiv.org/abs/https://doi.org/10.1142/S0129183102003760)
- [26] Andrey Malinin and Mark Gales. 2018. Predictive Uncertainty Estimation via Prior Networks. [arXiv:1802.10501 \[stat.ML\]](https://arxiv.org/abs/1802.10501)
- [27] Étienne Marcotte, Valentina Zantedeschi, Alexandre Drouin, and Nicolas Chapados. 2023. Regions of reliability in the evaluation of multivariate probabilistic forecasts. In *Proceedings of the 40th International Conference on Machine Learning (Honolulu, Hawaii, USA) (ICML '23)*. JMLR.org, Article 999, 47 pages.
- [28] Michael Mathieu, Camille Couprie, and Yann LeCun. 2016. Deep multi-scale video prediction beyond mean square error. [arXiv:1511.05440 \[cs.LG\]](https://arxiv.org/abs/1511.05440)
- [29] Mahdi Pakdaman Naeni, Gregory Cooper, and Milos Hauskrecht. 2015. Obtaining well calibrated probabilities using bayesian binning. In *Proceedings of the AAAI conference on artificial intelligence*, Vol. 29.
- [30] Sergiu Oprea, Pablo Martinez-Gonzalez, Alberto Garcia-Garcia, John Alejandro Castro-Vargas, Sergio Orts-Escolano, Jose Garcia-Rodriguez, and Antonis Argyros. 2022. A Review on Deep Learning Techniques for Video Prediction. *IEEE Transactions on Pattern Analysis and Machine Intelligence* 44, 6 (2022), 2806–2826. <https://doi.org/10.1109/TPAMI.2020.3045007>
- [31] Emanuel Parzen. 1999. Stochastic Processes.
- [32] David Radke, Anna Hessler, and Dan Ellsworth. 2019. Firecast: Leveraging Deep Learning to Predict Wildfire Spread. In *Proceedings of the 28th International Joint Conference on Artificial Intelligence (Macao, China) (IJCAI'19)*. AAAI Press, 4575–4581.
- [33] Olaf Ronneberger, Philipp Fischer, and Thomas Brox. 2015. U-Net: Convolutional Networks for Biomedical Image Segmentation. [arXiv:1505.04597 \[cs.CV\]](https://arxiv.org/abs/1505.04597)
- [34] Richard C Rothermel. 1972. *A mathematical model for predicting fire spread in wildland fuels*. Vol. 115. Intermountain Forest & Range Experiment Station, Forest Service, US ...
- [35] Helen R. Sofaer, Jennifer A. Hoeting, and Catherine S. Jarnevich. 2019. The area under the precision-recall curve as a performance metric for rare binary events. *Methods in Ecology and Evolution* 10, 4 (2019), 565–577. <https://doi.org/10.1111/2041-210X.13140> [arXiv:https://besjournals.onlinelibrary.wiley.com/doi/pdf/10.1111/2041-210X.13140](https://besjournals.onlinelibrary.wiley.com/doi/pdf/10.1111/2041-210X.13140)
- [36] David B Stephenson, Caio AS Coelho, and Ian T Jolliffe. 2008. Two extra components in the Brier score decomposition. *Weather and Forecasting* 23, 4 (2008), 752–757.
- [37] Steven H Strogatz. 2018. *Nonlinear dynamics and chaos: with applications to physics, biology, chemistry, and engineering*. CRC press.
- [38] O. Séro-Guillaume and J. Margerit. 2002. Modelling forest fires. Part I: A complete set of equations derived by extended irreversible thermodynamics. *International Journal of Heat and Mass Transfer* 45 (04 2002), 1705–1722. [https://doi.org/10.1016/S0017-9310\(01\)00248-4](https://doi.org/10.1016/S0017-9310(01)00248-4)
- [39] Matthew Thompson, Phil Bowden, April Brough, Joe Scott, Julie Gilbertson-Day, Alan Taylor, Jennifer Anderson, and Jessica Haas. 2016. Application of Wildfire Risk Assessment Results to Wildfire Response Planning in the Southern Sierra Nevada, California, USA. *Forests* 7, 12 (Mar 2016), 64. <https://doi.org/10.3390/f7030064>
- [40] Seth Tisue and Uri Wilensky. 2004. Netlogo: A simple environment for modeling complexity. In *International conference on complex systems*, Vol. 21. Citeseer, 16–21.
- [41] John Wainwright and George Francis Rayner Ellis. 1997. *Dynamical systems in cosmology*.
- [42] Ailian Wang, Weili Wu, and Junjie Chen. 2014. Social network rumors spread model based on cellular automata. In *2014 10th International Conference on Mobile Ad-hoc and Sensor Networks*. IEEE, 236–242.
- [43] Yunbo Wang, Zhifeng Gao, Mingsheng Long, Jianmin Wang, and S Yu Philip. 2018. Predrnn++: Towards a resolution of the deep-in-time dilemma in spatiotemporal

- predictive learning. In *International Conference on Machine Learning*. PMLR, 5123–5132.
- [44] Yunbo Wang, Mingsheng Long, Jianmin Wang, Zhifeng Gao, and Philip S Yu. 2017. Predrnn: Recurrent neural networks for predictive learning using spatiotemporal lstms. *Advances in neural information processing systems* 30 (2017).
- [45] A. L. Westerling, H. G. Hidalgo, D. R. Cayan, and T. W. Swetnam. 2006. Warming and Earlier Spring Increase Western U.S. Forest Wildfire Activity. *Science* 313, 5789 (2006), 940–943. <https://doi.org/10.1126/science.1128834> arXiv:<https://www.science.org/doi/pdf/10.1126/science.1128834>
- [46] S Hoya White, A Martin Del Rey, and G Rodríguez Sánchez. 2007. Modeling epidemics using cellular automata. *Applied mathematics and computation* 186, 1 (2007), 193–202.
- [47] Enze Xie, Wenhai Wang, Zhiding Yu, Anima Anandkumar, Jose M. Alvarez, and Ping Luo. 2021. SegFormer: Simple and Efficient Design for Semantic Segmentation with Transformers. arXiv:2105.15203 [cs.CV]
- [48] Suwei Yang, Massimo Lupascu, and Kuldeep Meel. 2021. Predicting Forest Fire Using Remote Sensing Data And Machine Learning. *Proceedings of the AAAI Conference on Artificial Intelligence* (03 2021). <https://doi.org/10.1609/aaai.v35i17.17758>
- [49] Yanzhu Zan, Da Li, and Xingzhen Fu. 2022. Emulation of Forest Fire Spread Using ResNet and Cellular Automata. In *2022 7th International Conference on Computer and Communication Systems (ICCCS)*. 109–114. <https://doi.org/10.1109/ICCCS55155.2022.9845891>
- [50] Richard Zinck and Volker Grimm. 2008. More Realistic than Anticipated: A Classical Forest-Fire Model from Statistical Physics Captures Real Fire Shapes. *The Open Ecology Journal* 1 (09 2008), 8–13. <https://doi.org/10.2174/1874213000801010008>

A OVERVIEW

• Literature Survey	B
– Models for forest fire modeling	B.1
– Cellular Automata in wildfire applications	B.2
• Background	C
– NetLogo Model	C.1
– Calibration Curve	C.2
– Next Day Wildfire Spread dataset	C.3
• DNN Characterization	D
– Design Rationale behind convLSTM-CA and conv-CA	D.1
– Qualitative Visualizations of DNN Forecasts	D.2
– Visualizing the DNN’s predictions using Empirical Stochastic Process	D.3
• Impact of macro-variance on the evaluation metrics	E
• Generalization study of ECE to other DNNs	F
• Long term predictions w.r.t stochastic process	G
• Asymptotic guarantees of MSE and ECE	H

B LITERATURE SURVEY

B.1 Models for forest fire modeling

Currently, forest fire spread models are categorized into three classes: empirical, semi-empirical, and physical. Empirical models, e.g., DNN modeling using remote sensing data [18], analyze fire data statistically without exploring combustion mechanisms. Semi-empirical models, often the preferred choice, like [7, 34] integrate physical laws, such as heat transfer, but necessitate resource-intensive ground surveys for calculating model parameters [7]. Physical models, involving complex equations for heat dynamics [38], are too complex for broad application. All these classes of models are deterministic and do not capture the stochastic nature of real-world fire dynamics.

B.2 Cellular Automata in wildfire applications

Cellular Automata (CA) models, with each pixel acting as an individual agent, offer a natural way to simulate stochastic interactions. These models, defined by discrete space and time, and marked by local spatial interactions, align well with the geographical nature of forest fires [13]. In CA-based forest fire models, each cell on fire is an agent capable of spreading the fire based on neighborhood interaction rules, leading to *emergent behaviors that mirror real-life fire propagation patterns* [2, 50]. CA models have been employed for various purposes in wildfire modeling, such as learning fire spread rules [49], learning parameters influencing agent interactions [22], and investigating chaos in fire evolution using Mean Field techniques [25].

C BACKGROUND

C.1 NetLogo Model

The simulation starts on a 64×64 grid, with each pixel initialized as a ‘tree’ or ‘no-tree’. Agents have heat values $q_{(i,j)}$ crucial for the heat transfer in forest fire evolution. Fire seeds, placed at randomized (or fixed) locations, provide initial heat to agents. The initial condition is set as $q_{(i,j)} = I_{seed} \times q_{threshold}$ for seed locations (i, j) , and $q_{(i,j)} = 0$ otherwise, where $q_{threshold}$ is the ignition threshold and I_{seed} amplifies seed heat values. A ‘tree’ agent accumulates heat from activated neighbors in its Moore neighborhood, in line with heat transfer mechanisms described by [34], following the equation:

$$q_{(i,j)}(t + \Delta t) = q_{(i,j)}(t) + \sum_{(k,l) \in N_R} \mathbf{1}_{(k,l)}(t) q_{(k,l)}(t) \quad (6)$$

The indicator function $\mathbf{1}_{(k,l)}(t)$ ensures only ‘fire’ state agents contribute to heat transfer. An agent’s heat value $q_{(i,j)}$ exceeding $q_{threshold}$ triggers a state change from ‘patch’ to ‘fire’, and then to ‘ember’ in the next time step. ‘Ember’ agents radiate heat at a rate of q_{die} to adjacent non-fire patches, gradually losing heat until radiation ceases. This process ends when ‘ember’ agents darken, indicating $q_{(i,j)}$ falling below a certain threshold, thus terminating heat radiation and transitioning to the ‘dead’ state.

C.2 Calibration Curve

Added interpretability to ECE using calibration curves. The calibration curve is an interpretable tool to intuitively understand the deviation between the model and the estimated probability in ECE. Given a set of frames (in a test dataset) $\{G_n\}_{n=1}^N$, where each G_n represents a grid of dimension $H \times W$, let $p_{n,i,j} = F(G_n)_{i,j} \in [0, 1]$ represent the forecasted probability by the classifier for each location (i, j) within the grid G_n . These probabilities $p_{n,i,j}$ are grouped into intervals I_k for $k = 1, 2, \dots, m$, partitioning the range $[0, 1]$ (e.g., $[0, 0.1]$, $(0.1, 0.2]$, etc.). A calibration curve is then constructed by plotting the predicted average probability $\bar{p}_k = \frac{1}{N_k} \sum_{n,i,j:p_{n,i,j} \in I_k} p_{n,i,j}$ for each

interval I_k against the observed empirical average $\bar{y}_k = \frac{1}{N_k} \sum_{n,i,j;p_{n,i,j} \in I_k} y_{n,i,j}$, where $y_{n,i,j}$ is the GT for the location (i, j) in grid G_n , and $N_k = |\{(n, i, j) : p_{n,i,j} \in I_k\}|$ represents the total number of predictions in interval I_k . Perfect calibration is indicated by the calibration curve forming a straight line, with an interpretable intuition backing the curve, out of all the predictions the DNN made with p x, x% actually burnt, tying down the metric to real-world actions.

C.3 Next Day Wildfire Spread dataset

Table 5: Summary of Observational Variables in the Next Day Wildfire Spread Dataset [16]

Observational Variable	Description
Elevation	Terrain height above sea level
Wind Direction	The direction from which the wind originates
Wind Speed	Velocity of the wind
Minimum Temperature	Lowest daily temperature
Maximum Temperature	Highest daily temperature
Humidity	Amount of water vapor in the air
Precipitation	Amount of rain, snow, etc., that falls
Drought Index	Measure of dryness indicating drought conditions
Vegetation	Vegetation indices indicating plant health and coverage
Population Density	Number of individuals per unit area
Energy Release Component (ERC)	Indicator of fire potential energy release

D DNN CHARACTERIZATION

D.1 Design Rationale behind convLSTM-CA and conv-CA

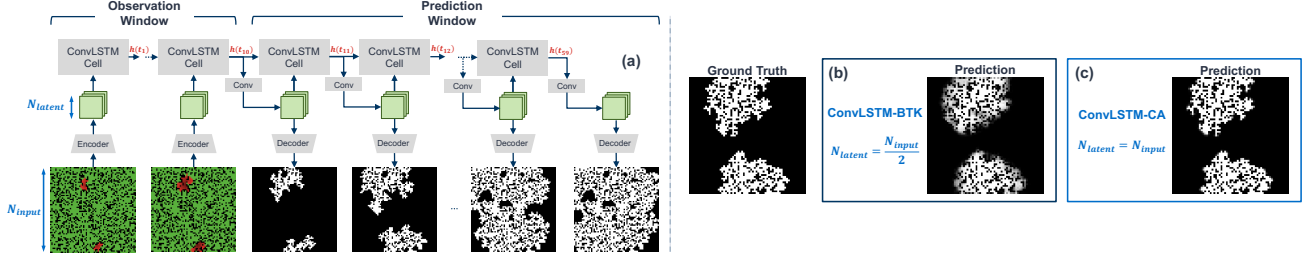


Figure 10: (a) Auto-regressive training of the DNN, (b) Softmax probability map from a convLSTM with a bottleneck, and (c) Softmax probability map from convLSTM-CA with no bottleneck.

The ConvLSTM architecture is chosen for its ability to efficiently model spatiotemporal systems, aligning well with the characteristics of the Forest-Fire system. Our modified version (see Figure 10.(a)), convLSTM-CA, places a ConvLSTM cell with a 3×3 kernel between an Encoder (with a 3×3 kernel) and a Decoder (with a 1×1 kernel). The Encoder takes an RGB image and transforms it into a latent tensor during a 10-timestep observation window. This tensor is then processed by the ConvLSTM cell, *maintaining its spatial dimensions*, before the Decoder produces a burnt map grid of softmax probabilities.

This design choice of preserving spatial dimensions is crucial. Reducing the spatial dimensions of the latent tensor is a popular design choice in video prediction models such as recurrent neural network-based [43, 44] and simple CNN-based models [10]. This reduction is often employed to decrease computational complexity and to capture essential spatial features while discarding less informative details. However, we observe that adding a bottleneck causes individual pixels (agents) to lose their identity. Maintaining these dimensions helps preserve each agent’s identity, a critical factor for developing a DNN that minimizes mis-calibrated forecasts arising from limited model capacity. For instance, as seen in Figure 10. (b), using a compressed latent dimension results in a forecast cloud around predictions for deterministic fire evolution scenarios, which does not accurately reflect the system’s true evolution. In contrast, as shown in Figure 10.(c) an uncompressed latent space yields predictions without a forecast cloud, aligning closely with the deterministic system’s true evolutionary rules. Conv-CA used in Section 5.3, is a version of Conv-AE [16] with the spatial bottleneck eliminated.

D.2 Qualitative Visualizations of DNN Forecasts

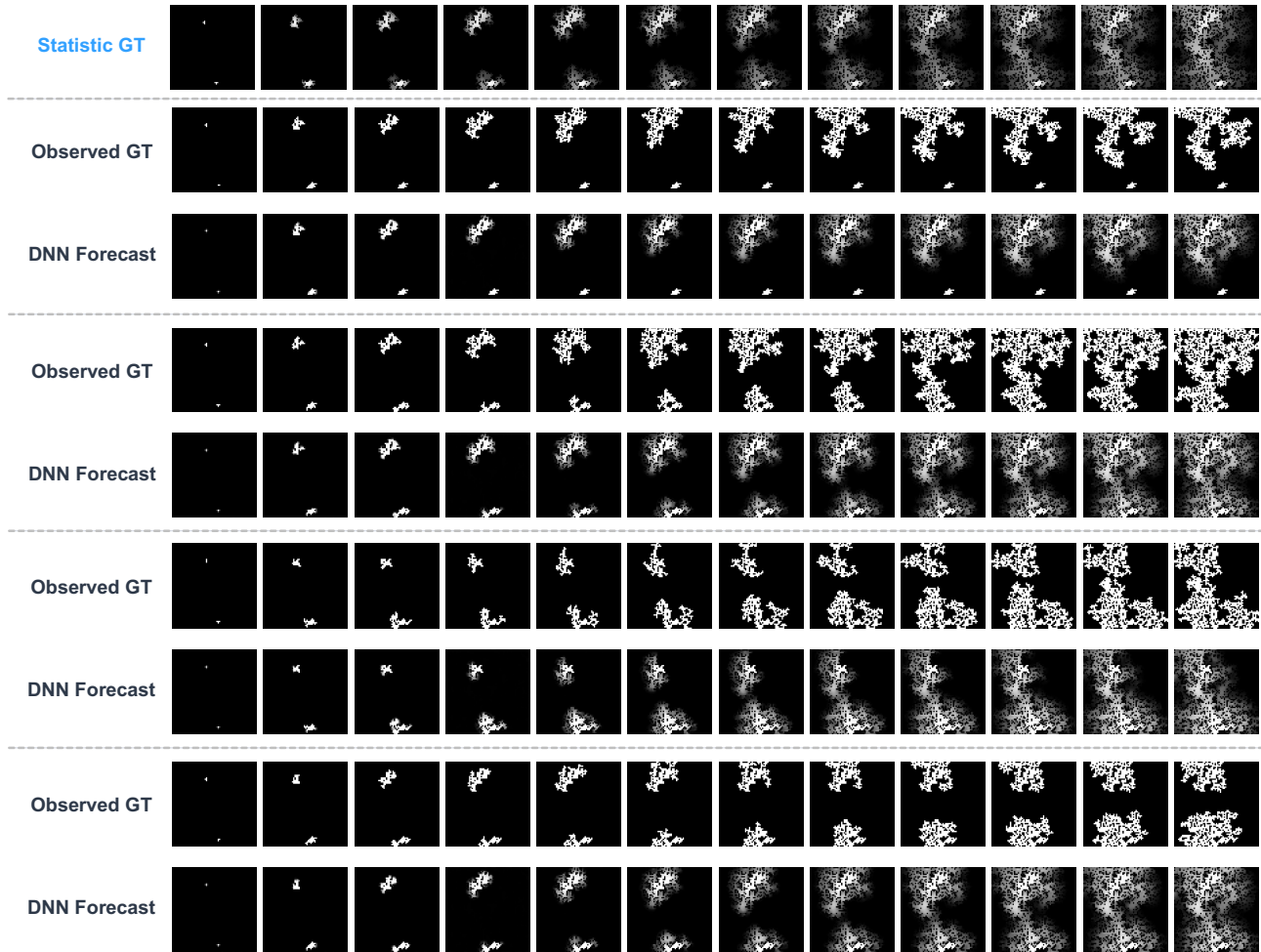


Figure 11: Qualitative Visualizations of the DNN's forecasts for four different MC simulations. Frames are shown every five time steps. The DNN observes the first 10 time steps (first 2 frames) and predicts the next 50 time steps (last 10 frames). We can observe the difference between the DNN's forecasts and the statistic GT, which arises because of the determinism that is injected into the DNN's predictions due to its observation of the first 10 frames of the fire evolution.

D.3 Visualizing DNN’s predictions using ESP

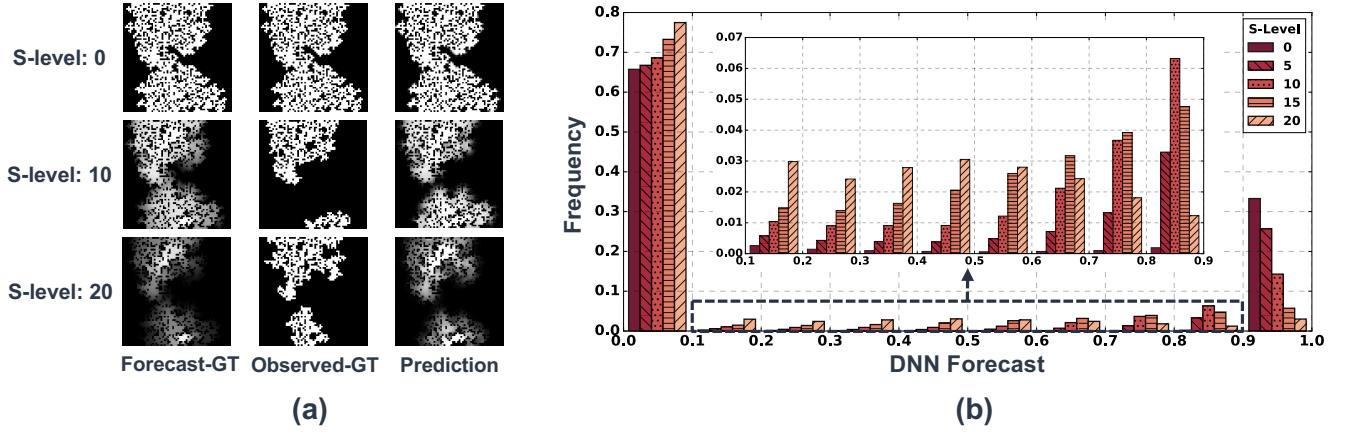


Figure 12: (a) Qualitative visualizations of forest-fire snapshots for different S-Level (one per row) showing statistic-GT, observed GT, and the corresponding DNN Prediction (raw forecast values); (b) Histogram shows the frequency of DNN’s forecast values for different S-Level values. We can observe that the DNN’s prediction becomes less confident with an increase in S-Level

Figure 12.a shows the DNN’s raw outputs, Statistic-GT, and Observed-GT (MC sample) for various S-levels, where higher S-levels correlate with greater ‘cloudiness’ in DNN output. Figure 12.b illustrates histograms of DNN predictions across 1000 simulations for each S-Level. In deterministic settings, predictions are mainly binary (1 or 0), but at S-Level 20, predictions span the 0-1 range, indicating increased predictive uncertainty in highly stochastic scenarios. This ability to learn and predict stochastic fire evolution is linked to the use of BCE loss, which ensures calibrated forecasts by learning the true probability distribution of the process [12].

E IMPACT OF MACRO-VARIANCE ON THE EVALUATION METRICS

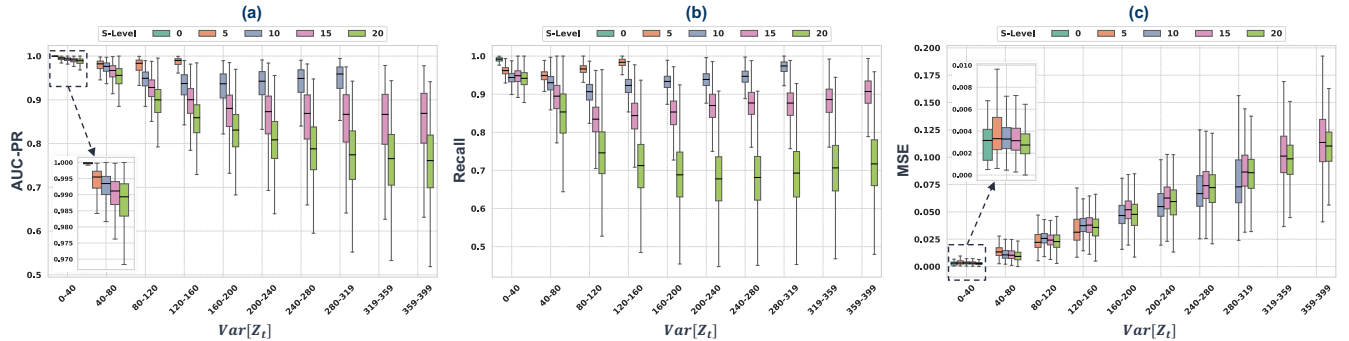


Figure 13: Impact of macro-variance $Var[Z_t]$ on the performance of the DNN using (a) AUC-PR (b) Recall, and (c) MSE.

We use five different test cases with S-levels (0, 5, 10, 15, 20) and feed them to the trained DNNs operating at the corresponding S-levels, ensuring the training and testing S-levels match. Figure 13.a and b illustrate the inverse monotonic relationship between DNN performance (AUC-PR, Recall) and system macro-variance ($Var[Z_t]$), with the confidence width of these metrics widening as $Var[Z_t]$ increases. In contrast, as shown in Figure 13.c, MSE exhibits less sensitivity to the macro-variance, displaying a monotonic relationship with $Var[Z_t]$. The second component of the Brier Score Decomposition (see Equation 4), $E[Var(O|F)]$, quantifies the portion of total outcome variance unexplained by the forecasts, representing inherent uncertainty, which shows up in Figure 13.c.

F GENERALIZATION STUDY OF ECE TO OTHER DNNs

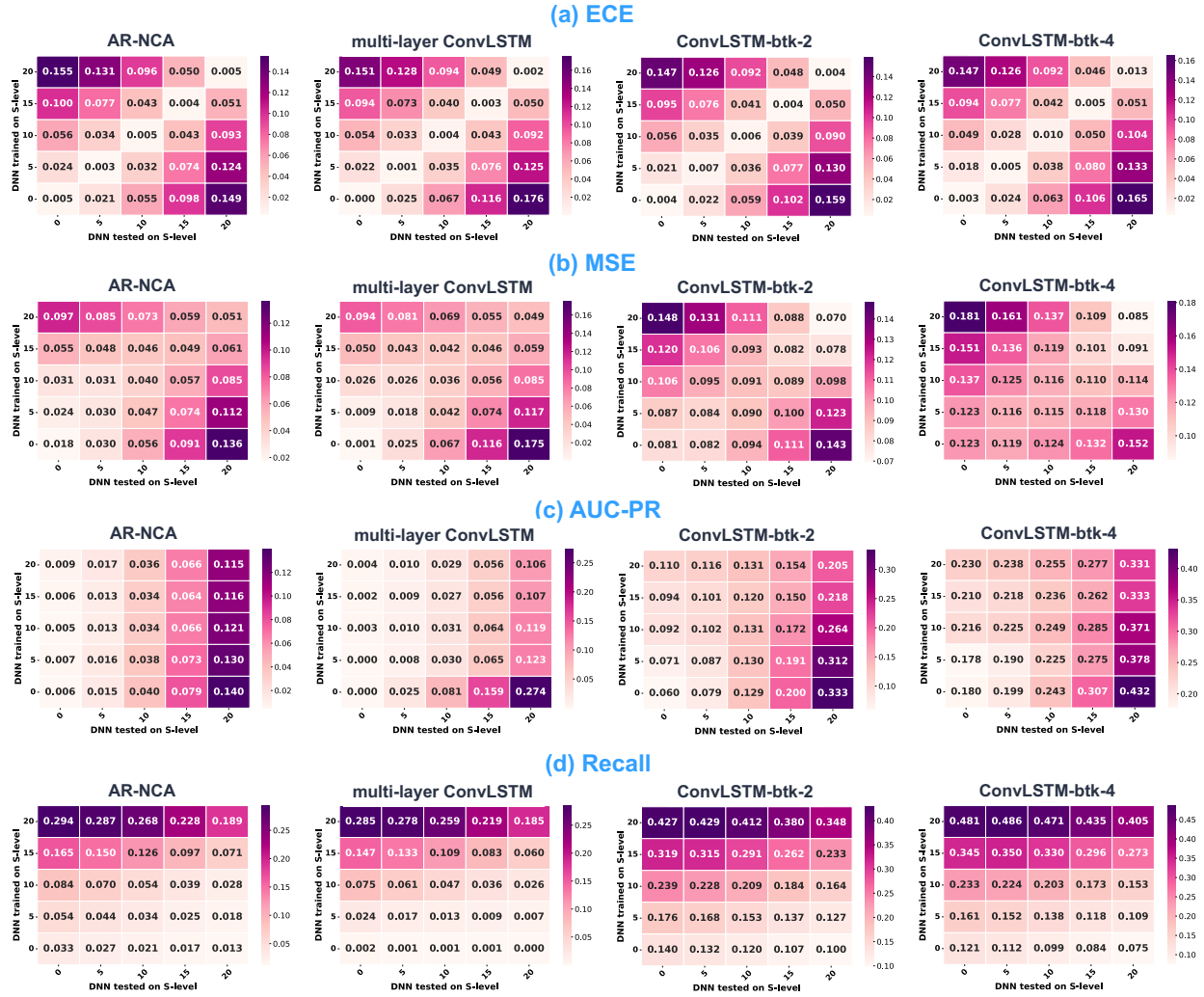


Figure 14: Evaluation metric scores for four different DNNs, from strongest (leftmost) to weakest (rightmost) using evaluation metrics (a) ECE, (b) MSE, (c) AUC-PR, and (d) Recall. While MSE, AUC-PR, Recall depict marked degradation in performance, ECE remains fairly stable, though slight increase is observed. In general, ECE shows lower variation, indicating that it has a lower discriminating power.

Details about the DNN Architectures: (1) AR-NCA [20]: AR-NCA involves a recurrent cellular attention module that couples long short-term memory (LSTM) and cellular self-attention, (2) multi-layer ConvLSTM (num_layers=2), (3) convLSTM-btk-2: convLSTM with a spatial bottleneck that downsamples by 2, (4) convLSTM-btk-4: convLSTM with a spatial bottleneck that downsamples by 4. In the order of DNN strength $1 \approx 2 > 3 > 4$.

G LONG TERM PREDICTIONS WRT STOCHASTIC PROCESS

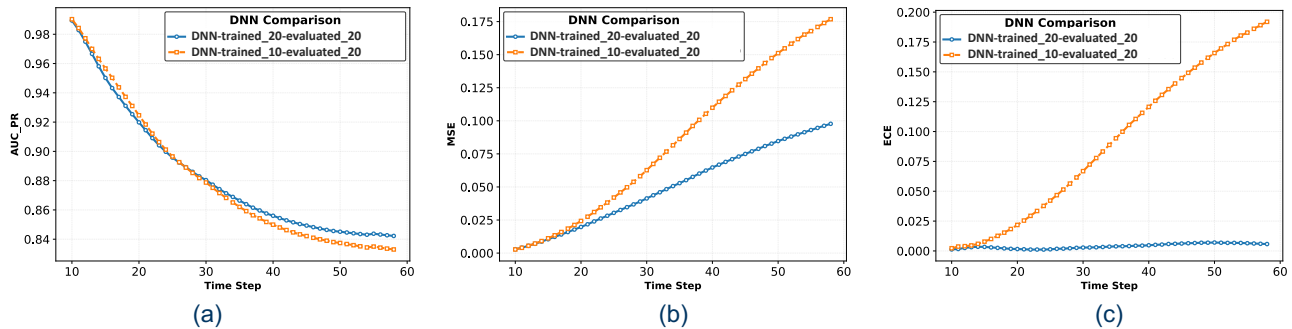


Figure 15: DNNs trained on S-Level 10 (orange) and S-Level 20 (blue) and evaluated on S-Level 20. Scores reported by evaluation metrics (a) AUC-PR, (b) MSE, and (c), ECE. Since each DNN has learnt different stochastic interactions, divergence in DNN-S-Level 10 can be observed in ECE which assesses fidelity to stochastic process.

In this experiment we evaluate what happens when the DNN learns from one s-level and is evaluated on the other. In this specific example, one DNN is trained on S-Level 20 and the other is trained on S-Level 10. They are both evaluated on S-Level 20. Figure 15 shows the performance of the two DNNs reported by AUC-PR, MSE, and ECE. AUC-PR doesn't show any difference between the two DNNs, as it's not evaluating the statistic. MSE and BCE show visible difference. ECE shows the steepest difference because the DNN learnt a different noisy interaction rule, affecting the probabilistic accuracy. The system variance common in both test cases, reduces the gap in MSE.

H ASYMPTOTIC GUARANTEES OF MSE AND ECE

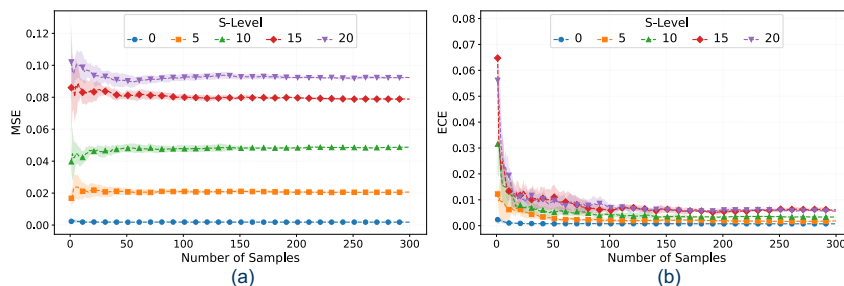


Figure 16: Testing the asymptotic guarantees of MSE and ECE. Each sample is a grid of predictions at $t=59$ in the test split of the synthetic forest dataset. As the number of samples increase in the calculation of MSE and ECE, they both converge. The MSE converges to a value that incorporates the $Var(Z_t)$, while the ECE converges to a low value as it excludes the impact of $Var(Z_t)$. We can observe, that for the asymptotic guarantees to kick in, sufficient number of samples are required.